Perovskite-Type Oxide Membranes for the Oxidative Coupling of Methane

Sherman J. Xu and William J. Thomson
Dept. of Chemical Engineering, Washington State University, Pullman, WA 99164

A series of ion-conducting perovskites of the form $[La_{1-x}A_x][Co_{0.2}Fe_{0.8}]O_{3-\delta}$ (x = 0.4, 0.6 for A = Sr; x = 0.8 for A = Ba) were investigated for their use as a catalytic membrane for the oxidative coupling of methane (OCM). A-site cations consisting of $La_{0.4}Sr_{0.6}$ and $La_{0.2}Ba_{0.8}$ produce materials with the highest oxygen fluxes and result in C_{2+} selectivities of 50% at 1,098 K, which are significantly higher than those achieved with a powdered catalyst in a packed-bed reactor configuration. Selectivities in these materials appear to be limited by high oxygen ion recombination rates that compete for oxygen with the desired coupling reaction(s). The results also indicate that oxygen fluxes are not limited by diffusion, but by surface exchange rates at the oxygen-lean side of the membrane. The study on stability of these materials showed that all three perovskites could be reduced in a pure methane or ethane stream at 1,023 K, but they were totally stable under reaction conditions where oxygen is present.

Introduction

The catalytic oxidative coupling of methane (OCM) can occur over a wide variety of catalysts, including alkali-metal-promoted alkaline-earth-oxide catalysts such as Li-, Na-, and K-promoted MgO and CaO oxides (Choudhary et al., 1994; Baronetti et al., 1993; Grzybek et al., 1993; Peng and Stair, 1991) and rare-earth metal oxides such as La_2O_3, Sm_2O_3, and Y_2O_3 (Lacombe et al., 1995; Buyevskaya et al., 1994; Squire et al., 1994; Tang et al., 1994; Kaminsky et al., 1992; Dobois et al., 1990). However they all suffer from rather low selectivities at the high conversions required for commercial importance, typically producing yields no higher than 20%. It is generally agreed that dissociated oxygen is a necessary requirement for the generation of methyl radicals and the subsequent coupling of methyl radicals to ethane and ethylene (Reyes et al., 1993; Lunsford, 1989; Driscoll et al., 1987). Because of this Xu (1994) was prompted to examine the OCM catalytic activity of oxygen ion-conducting perovskites such as $La_{1-x}Sr_xCo_{1-y}Fe_yO_{3-\delta}$ (LSCF) in a packed-bed reactor. Although their activities were inferior to the more conventional OCM catalysts, the results were sufficiently encouraging to warrant a study of their efficiency as OCM catalytic membranes.

As pointed out by Steele (1992) in a survey of oxygen-ion conductors and their applications, highly defective perovskite mixed conductors can become disordered at elevated temperatures to produce materials that can exhibit very high oxygen-ion conductivity. The partial substitution of both A and B cations in the perovskite (ABO_3) lattice structure with cations of different valencies has been generally recognized to facilitate the formation of oxygen vacancies and the enhancement of oxygen-ion conductivity. In a study of the conductivity of $La_{1-x}Sr_xCo_{1-y}Fe_yO_{3-\delta}$ perovskite-type oxides, Teraoka et al. (1988, 1985) found that partial substitutions of Sr for La and Fe for Co dramatically increased the ionic–electronic conductivity of these oxides. For instance, the oxygen permeation rates through $La_{1-x}Sr_xCo_{0.4}Fe_{0.6}O_{3-\delta}$ at 1,146 K increased dramatically from 0.0 to 17.7 mmol/(m^2·s) as x was increased from 0 to 1. However, La cations at A sites are necessary for the stability of this perovskite at high temperatures (ten Elshof et al., 1995b). A variety of perovskite oxides has also been reported as promising OCM catalysts that are known to exhibit substantial oxygen-ion conductivity under conditions of interest and are quite active and selective in converting methane into dimeric species (C_2H_4 and C_2H_6) (Alcock et al., 1992; Barrault et al., 1992; Zhang and Baerns, 1992). During a study of the reactivity of structural oxygen in connection with the structure of various mixed oxides obtained by substituting A and B site cations of $LaCoO_{3-\delta}$ with alkaline earth metals (Mg, Ca, Sr, and Ca) and transition

Correspondence concerning this article should be addressed to W. J. Thomson.

metals (Fe, Ni, and Cu), Hayakawa et al. (1992) found that nonperovskite $Co_{0.8}Fe_{0.2}O_{3-\delta}$ had no activity at all for the OCM reaction, while perovskites such as $BaCo_{0.8}Fe_{0.2}O_{3-\delta}$, $La_{0.6}Ba_{0.4}Co_{0.8}Fe_{0.2}O_{3-\delta}$ and $SrCo_{0.8}Fe_{0.2}O_{3-\delta}$ showed relatively high activity to C_{2+} hydrocarbons. Additionally, according to a recent study by Lin and Zeng (1996), the partial substitution of A site cations as in $La_{0.8}Sr_{0.2}CoO_3$ improved the OCM activity and selectivity much more than the complete A site substitution and partial B site substitution as in $SrCo_{0.8}Fe_{0.2}O_3$. The results here implied that the formation of hypervalent metal ions such as Co^{4+} and Fe^{4+} and the disordering of lattice oxygen in the perovskite-crystal structure under elevated temperatures played important roles in the OCM reaction.

The preceding observations suggest that nonporous oxygen-ion-conducting perovskite oxides have potential as OCM catalytic membrane reactors using air as an economical oxygen source. Since the pioneer work by Fujimoto and coworkers (Omata et al., 1989), this type of dense membrane reactor for the OCM reaction has drawn some attention recently by ten Elshof et al. (1995a) and Andersen et al. (1994). The behavior of dense oxide membrane reactors was simulated by Wang and Lin (1995) based on the kinetic equations for OCM reaction derived from the following mechanism written in the Kröger-Vink notations (Kröger, 1964):

$$0.5O_2 + V\ddot{O} \xleftrightarrow{k_1/k_{-1}} O_O^{\times} + 2h^{\cdot} \quad \text{(A)}$$

$$CH_4 + h^{\cdot} + 0.5O_O^{\times} \xrightarrow{k_2} \cdot CH_3 + 0.5H_2O + 0.5V\ddot{O} \quad \text{(B)}$$

$$\cdot CH_3 + \frac{x}{2}O_2 \xrightarrow{k_3} CO_2 \quad \text{(C)}$$

$$2\cdot CH_3 \xrightarrow{k_4} C_2H_6 \quad \text{(D)}$$

$$C_2H_6 + h^{\cdot} + 0.5O_O^{\times} \xrightarrow{k'_2} \cdot C_2H_5 + 0.5H_2O + 0.5V\ddot{O} \quad \text{(E)}$$

$$\cdot C_2H_5 + \frac{x}{2}O_2 \xrightarrow{k'_3} 2CO_2. \quad \text{(F)}$$

As illustrated in this simplified mechanism, methane is adsorbed and reacts with the lattice oxygen ion ($O_O^{\times}$) of the catalyst to form methyl radicals at the reaction side of the membrane (Step B). Two methyl radicals then couple to form C_2 product into the gas phase in Step D. The oxygen vacancies ($V\ddot{O}$) generated in Step B are filled by gas oxygen with the overall surface reaction at the oxygen side represented in Step A. All of the combustion reactions, Steps C and F, were assumed to take place only in the gas phase. Applying the kinetic data obtained on a Li/MgO catalyst (Tung and Lobban, 1992), the results of this simulation showed that a commercial high C_{2+} yield (75%) could be achieved with a dense oxide membrane reactor under the conditions given in Table 1. Such a membrane was constructed and studied by ten Elshof et al. (1995a). They achieved a 62.6% C_{2+} hydrocarbon selectivity with a $La_{0.6}Sr_{0.4}Co_{0.8}Fe_{0.2}O_3$ perovskite membrane at 1153 K and $P_{CH_4} = 93$ kPa. Under such conditions, the rate of C_2 production was 0.27 mmol/m^2·s, and a 10% H_2 selectivity was observed. It can be inferred from these results that too high a temperature might bring about excess oxygen-ion supply for OCM reaction as well as thermal decomposition of methane. They also observed that strontium segregation occurred after the membrane disk was treated in an air/CH_4 gradient at 1,153 K.

Table 1. Values of Parameters Used in Simulation of OCM in Membrane Continuously Stirred-Tank Reactor

Membrane area	6.28×10^{-3} m^2
Temperature	1,023 K
Reaction and oxygen chamber pressures	101 kPa
Methane flow rate at reaction chamber	0.22 mmol/s
Air flow rate at oxygen chamber	1.12 mmol/s
Oxygen permeation flux	2.90 mmol/(m^2·s)
C_2 production rate	8.44 mmol/(m^2·s)
C_2 selectivity required	> 82.5%

Source: Wang and Lin (1995).

In order to achieve commercial viability it is necessary that suitable perovskite formulations be developed that have high oxygen-ion conductivities as well as good stability to the presence of reducing gases and that catalytic membrane conditions be optimized to produce high C_{2+} selectivities at reasonably high rates. Consequently, three perovskite membranes known for their high oxygen-ion conductivity, $La_{0.6}Sr_{0.4}Co_{0.2}Fe_{0.8}O_{3-\delta}$ (LSCF-6428), $La_{0.4}Sr_{0.6}Co_{0.2}Fe_{0.8}O_{3-\delta}$ (LSCF-4628), and $La_{0.2}Ba_{0.8}Co_{0.2}Fe_{0.8}O_{3-\delta}$ (LBCF-2828), have been studied with the objective of increasing C_{2+} selectivities above the 12–17% values obtained in a packed-bed configuration (Xu, 1994) and to determine how these materials could have sufficient stability when exposed to reducing gases such as methane and ethane. The effects of reaction variables were studied in an attempt to quantify their influence on C_{2+} selectivity. In addition, another objective of this study was to identify the rate-determining step(s) under OCM reaction conditions.

Experimental Studies

Preparation of catalysts

The perovskite materials were prepared at the Battelle Pacific Northwest National Laboratory (PNNL) using the glycine–nitrate combustion synthesis technique (Chick et al., 1990). Reagent-grade La, Sr, Ba, Co, and Fe nitrates were dissolved in deionized water according to each of the selected compositions within the system $La_{1-x}A_xCo_{0.2}Fe_{0.8}O_{3-\delta}$ ($x = 0.4$, 0.6 for A = Sr; $x = 0.8$ for A = Ba). After glycine was added as a fuel and complexant, the solution at approximately one molar (cation basis) concentration was boiled to evaporate excess water and further heated until the viscous liquid ignited and underwent self-sustaining combustion, producing 0.02 moles of perovskite product by burning approximately 4×10^{-5} m^3 of the precursor solution. The resulting ash was then calcined in air at 1,123 K for 12 h and compressed into disks, 17 mm diameter and 2–3.5 mm thick, using uniaxial pressure (55 MPa) followed by isostatic pressure (138 MPa). The pressed compacts were then sintered in $MoSi_2$ furnaces at 1,473 K for 2 h using heating and cooling rates of 5 K/min in order to achieve single-phase and fully densified disks (> 95% of theoretical).

Membrane reactor assembly

Figure 1 shows a sketch of the experimental apparatus. The membrane reactor assembly consisted of two sets of mullite tubes surrounding a quartz tube and separated by the per-

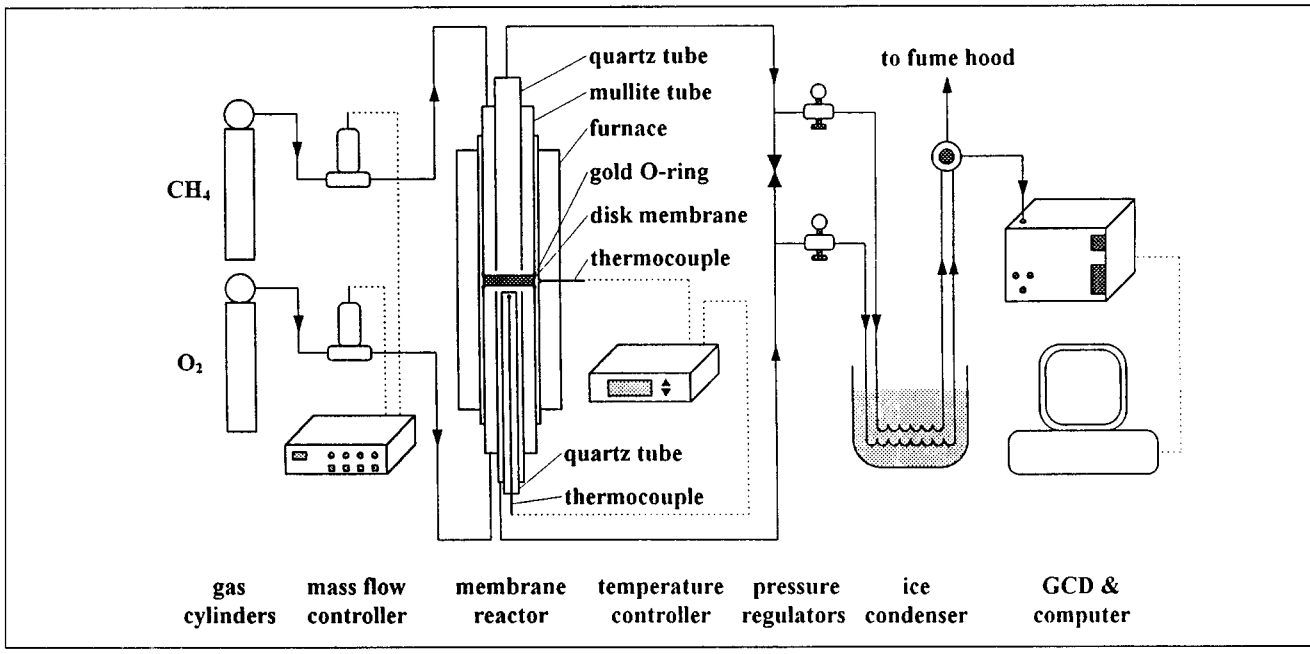

Figure 1. Membrane reactor assembly.

ovskite catalyst, which was shaped into a disk with a thickness of 2–3.5 mm and a diameter of 17 mm. Gold gaskets were used to obtain effective seals between the disk and the walls of the mullite tubing, and pressures as high as 300 kPa could be tolerated by placing the assembly in compression with the use of spring clamps. The inlet gas flows were controlled by Matheson Multi-Channel Mass Flow Controllers (Model 8274), which maintain stable and constant flow and eliminate the influence of changes in reactor working pressures that are maintained by two HP back-pressure regulators. Either pure oxygen or oxygen–helium flows [331 mmol/$(m^2 \cdot s)$] were introduced into the upper chamber, just above the catalytic disk in order to minimize gas–solid mass-transport effects. Methane was fed to the lower chamber in the same fashion [166 mmol/$(m^2 \cdot s)$] and this stream was analyzed by means of an HP Model 1800A GCD, which has a mass spectrograph as the detector. The reactor assembly was surrounded by a vertical-tube furnace, and temperatures were measured by a type K thermocouple encased in a quartz tube to avoid the combustion of methane and C_{2+} products, which would otherwise be caused by the direct contacting of thermocouple materials and reactant gases. A Eurotherm Microprocessor Temperature Controller (Model 810) was used to maintain stable and isothermal reaction conditions, and the temperature at the perovskite membrane disk was controlled to within ± 1 K of the setpoint.

Hydrogen in the effluent stream was analyzed by a Model 111-H Carle Analytical Gas Chromatograph (GC) equipped with a 1.83-m molecular sieve 5A, 80/100-mesh column and a Hydrogen Transfer Tube (HTT) operated at 873 K. N_2 (3.72×10^{-2} mmol/s) and He (2.01×10^{-2} mmol/s) were used as carrier gases.

Perovskite stability measurements

The stability of the perovskite oxides resulting from methane and ethane reduction effects were characterized by using *in situ* "dynamic X-ray diffraction" (DXRD). The equipment consists of a Siemens D-500 θ-2θ powder diffractometer equipped with a Co Kα_1 (1.7890 Å) source of radiation, a flowthrough, Anton-Parr hot stage encased in the middle of a reaction chamber, and a position-sensitive detector capable of rapid scanning (60 deg/min) at high resolution of 0.01 deg. A thin layer (less than 0.2 mm) of perovskite oxide powder was placed on the top of a platinum strip, which is electrically heated. A type-S thermocouple attached to the strip is used to monitor and control the temperature by means of Microstar Temperature Controller Model 828D, by which a multiloop heating program can be run for *in situ* temperature ramping experiments. DXRD runs were conducted at temperatures from 1,008 K to 1,118 K, with a heating rate of 1.2 K/min and with gas flows (0.11 mmol/s) of methane, ethane, and methane–oxygen mixtures.

Procedures

After the membrane disk was loaded, the reactor was heated to 1,098 K at 15 K/min with helium flowing through both sides of the membrane at a rate of 414 mmol/$(m^2 \cdot s)$ to prepare an oxygen-free environment in order to prevent the order–disorder phase change of perovskite oxides, which only takes place in an oxygen environment and at temperatures less than 973 K (Kruidhof et al., 1993). The effectiveness of the gold gasket seal was evaluated by holding the temperature at 1,098 K for 20 min and then comparing the inlet and exit flows in both chambers. Disk integrity was also verified by introducing N_2 and Ar on either side of the disk and then analyzing for Ar in the exit N_2 stream. This same procedure was followed whenever the temperature was changed or whenever different gases were used during the course of the experimental investigation. In order to monitor any deterioration in the oxygen-ion conductance, periodic measurements of the oxygen permeability were also conducted by introducing O_2 and N_2 to the different chambers of the reactor and

analyzing for O_2 in the effluent N_2 stream. During the activity tests, the total oxygen permeation rate was calculated from an O balance. The disk catalytic performances were evaluated in terms of C_{2+} activity—the production rate of C_{2+} hydrocarbons, which is defined as

$$r_{C_{2+}} = \frac{\text{Outlet flow rate of } C_{2+} \text{ hydrocarbons}}{\text{Membrane disk surface area}} \text{ [mmol/(m}^2\cdot\text{s)]}$$

and in terms of selectivity to C_{2+} hydrocarbons, which is defined as

$$S_{C_{2+}} = 100\% \times \frac{\text{Moles of } CH_4 \text{ converted to } C_{2+} \text{ hydrocarbons}}{\text{Moles of } CH_4 \text{ converted to all carbon products}}.$$

The flow rates of methane and oxygen were both varied to ensure that reaction rates did not influence C_2 production rates, thus eliminating gas–solid mass transfer as a rate-determining step. At these flow rates, methane conversions were low, and thus the methane pressures at the methane side of the membrane were essentially constant. Methane conversions were kept below 3% for all experiments, thus allowing for accurate and repeatable measurements of C_2 production rates.

Results and Discussion

Combustion reactions

In order to confirm the hypothesis that the combustion of C_{2+} products, which is the primary side reaction, takes place in the gas phase, experiments were conducted in the membrane reactor as well as in a tubular fixed-bed reactor. These experiments were carried out by feeding a 50:50 mix of C_2H_6 and O_2 (diluted with helium) to the same side of an LSCF-6428 disk and then comparing the results with identical "blank" experiments where the perovskite was replaced by an α-Al_2O_3 disk. These results are shown in Table 2, and it is readily apparent that with the exception of the lowest temperature where CO_x concentrations are quite small, combustion rates (as measured by CO_x yields) are consistently *higher* in the blank experiments. This demonstrates that combustion takes place in the gas phase, and the lower CO_x yields with the perovskite disk are due to the competitive OCM reaction on the perovskite surface. Similar experiments were carried out in a fixed-bed tubular reactor, using a samarium–lithium-promoted MgO catalyst. Again, with this superior OCM catalyst (Xu, 1994), CO_x yields are *lower* than in a blank quartz tube (Figure 2). The conclusion that C_{2+} combustion occurs in the gas phase is consistent with comparative reaction rates reported by Feng et al. (1991). These results present a strong argument for the use of a catalytically active membrane reactor to supply oxygen ions from the nonreactive side of the membrane for methane activation, and thus to prevent C_{2+} combustion caused by gas-phase oxygen.

Table 2. CO_x Yield for Ethane Combustion in Membrane Reactor

Temp. K	Al_2O_3 Disk* %	LSCF-6428* %	Al_2O_3 Disk** %	LSCF-6428** %
1,023	0.24	0.34	1.12	0.77
1,048	2.95	1.32	8.42	5.75
1,073	13.98	9.68	26.61	27.14
1,098	35.06	31.69	41.72	41.87

*Inlet gas flow rates [mmol/(m^2·s)]: C_2H_6 = 82.8, O_2 = 82.8, He = 1,243.
**Inlet gas flow rates [mmol/(m^2·s)]: C_2H_6 = 82.8, O_2 = 82.8, He = 828.

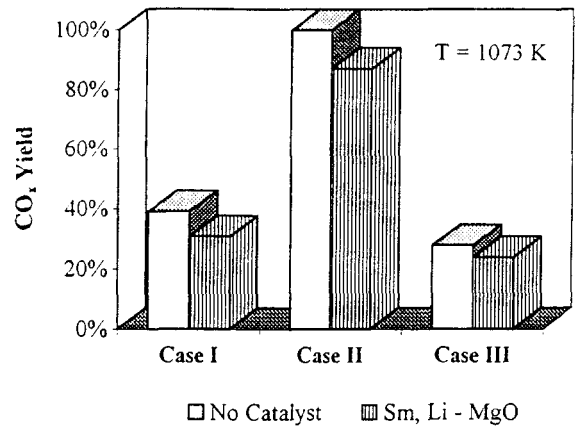

Figure 2. CO_x yields for C_2H_6 combustion: quartz-tube fixed-bed reactor.

The inlet gas flow rates (mmol/s) are: Case I: $C_2H_6 = 7.44 \times 10^{-3}$, $O_2 = 7.44 \times 10^{-3}$, $He = 5.95 \times 10^{-2}$; Case II: $C_2H_6 = 3.72 \times 10^{-3}$, $O_2 = 1.12 \times 10^{-2}$, $He = 5.95 \times 10^{-2}$; and Case III: $C_2H_6 = 3.72 \times 10^{-3}$, $O_2 = 3.72 \times 10^{-3}$, $He = 8.93 \times 10^{-2}$.

Methane surface activation and its effect on oxygen-ion conductivity and recombination

At the membrane surface on the reactive side of the membrane reactor, oxygen ions ($O_O^{\times}$) are competitively consumed by two reactions—methane activation (Reaction G) and recombination of oxygen ions (Reaction H) (Wang and Lin, 1995; Bouwmeester et al., 1994):

$$2CH_4 + 2h^{\cdot} + O_O^{\times} \rightarrow 2\cdot CH_3 + H_2O + V\ddot{O} \qquad \text{(G)}$$

$$2O_O^{\times} + 4h^{\cdot} \rightarrow O_2 + 2V\ddot{O}. \qquad \text{(H)}$$

Because the gaseous oxygen produced in Reaction H could further react with methyl radicals and C_{2+} products to form CO_x, a high oxygen-ion flux can increase OCM activity, but does not necessarily improve selectivity. A set of experiments was conducted at 1098 K on LSCF-6428 with different oxygen pressures at the oxygen side of the disk and with either N_2 or CH_4 on the oxygen-lean side of the membrane. As can be seen in Table 3, with methane present no improvement was observed in C_2 selectivity (S_{C_2}) or in the C_2 production

Table 3. Catalytic Performances of LSCF-6428 and Oxygen Flux as a Function of $P_{O_2}^*$

P_{O_2} kPa	$S_{C_2H_4}$ %	$S_{C_2H_6}$ %	S_{C_2} %	r_{C_2} mmol/(m^2·s)	J_{O_2} (with CH_4) mmol/(m^2·s)	J_{O_2} (with N_2) mmol/(m^2·s)
61	6.00	22.59	28.60	0.17	1.70	0.54
81	6.44	21.75	28.19	0.19	1.99	0.55
101	7.99	18.47	26.46	0.23	2.60	0.57

*LSCF-6428, T = 1.098 K, F_{CH_4} = 166 mmol/(m^2·s).

Table 4. Comparison between Measured and Calculated O_2 Flux Increases as a Function of $P^*_{O_2}$

P_{O_2} (kPa)	P'_{O_2} (kPa)	J_{O_2}/J_{O_2} (61 kPa)**	J_{O_2}/J_{O_2} (61 kPa)†
61	0.221	1	1
81	0.224	1.015	1.049
101	0.230	1.041	1.084

*LSCF-6428, O_2/N_2 gradient, $T = 1{,}098$ K, $F_{CH_4} = 166$ mmol/(m²·s).
**Calculated from measured oxygen flux with nitrogen listed in Table 3.
†Calculated according to Eq. I.

rate as the oxygen pressure was elevated from 61 kPa to 101 kPa.

On the other hand, when N_2 is present the oxygen flux drops by factors of $3 \sim 4$, indicating that oxygen-ion transport here is limited by surface-ion coupling (Reaction H). The values of the oxygen flux in the presence of N_2 are somewhat less than the $0.50 \sim 0.75$ mmol/(m²·s) measured by ten Elshof et al. (1995a) on LSCF-6482 with air/He gradient at 1,153 K. Assuming diffusional limitations, the maximum ionic conductivity through mixed conducting oxides can be estimated from the equation derived by Ling et al. (1993) from Wagner's equations (Wagner, 1951):

$$J_{O_O^\times}^{\max} = \frac{\sigma_t RT}{16F} \frac{\Delta(\ln P_{O_2})}{\Delta X}, \qquad \text{(I)}$$

where, $\sigma_t = \sigma_{O_O^\times} + \sigma_{e^-}$ is the total conductivity; T is temperature in K; R is the gas constant; F is the Faraday constant; and $[\Delta(\ln P_{O_2})]/\Delta X$ is the driving force across the membrane. According to this equation, the oxygen flux is proportional to $\ln(P_{O_2}/P'_{O_2})$ at constant temperature, where P_{O_2} and P'_{O_2} are oxygen pressures at the oxygen and reaction membrane sides, respectively. As can be seen in Table 4, as P_{O_2} increases from 61 to 101 kPa, the measured oxygen flux increases are lower than the values calculated from Eq. I, another indication that the oxygen-ion conducting process in the O_2/N_2 experiments is limited by surface-ion coupling. This is also consistent with the observations of ten Elshof et al. (1995a) with an LSCF-6482 membrane. However, when CH_4 is present at this surface, the OCM reaction occurs and its rate is higher than either of these two surface-rate steps in the presence of N_2, and consequently, the oxygen flux through the membrane increases. The fact that the calculated O_2 flux increases with P_{O_2} is due to the fact that the OCM rate is also dependent on the oxygen-ion concentration (Zhang and Baerns, 1992). However, in view of the fact that selectivities remain essentially constant, it appears that the oxygen transport rate through the membrane is still higher than the surface rate and thus, gaseous oxygen still manages to form via Reaction H. Thus, selectivity improvement can only occur by increasing the OCM catalytic activity or by lowering the oxygen-ion conductivity. Of course, if the latter is chosen, selectivity improvement will occur at the expense of C_{2+} production rate and would probably be impractical.

Effect of P_{CH_4}

The response of the OCM reaction parameters to increases in P_{CH_4} are shown in Figure 3 for LSCF-4628, LSCF-6428, and LBCF-2828. As can be seen in Figure 3a, the selectivities of LSCF-4628 and LBCF-2828 were both 50% at $P_{CH_4} = 101$ kPa. This is a dramatic improvement over the 12–17% values measured in the packed-bed reactor under comparable reaction conditions ($T = 750 \sim 850$°C, space velocity = 186 mmol/kg catalyst·s, $CH_4/O_2 = 25$), with methane conversion ranging from 2.9% to 4.1% (Xu, 1994). The C_{2+} production rates for these two membranes were, respectively, 0.67 and 0.89 mmol/(m²·s) (Figure 3b), which is a factor of 7 higher than the measured rates (on a per unit area basis) in the packed-bed reactors. Note that the concentration of oxygen detected in the outlet gas leaving the methane side of the membrane (Figure 3c) increases significantly as CH_4 pressure is reduced. This points to the presence of oxygen-ion recombination at this side of the membrane and also accounts for the lower selectivities at low methane pressures. That is, low methane pressures lower the OCM rate, and therefore the recombination rate occurs to a

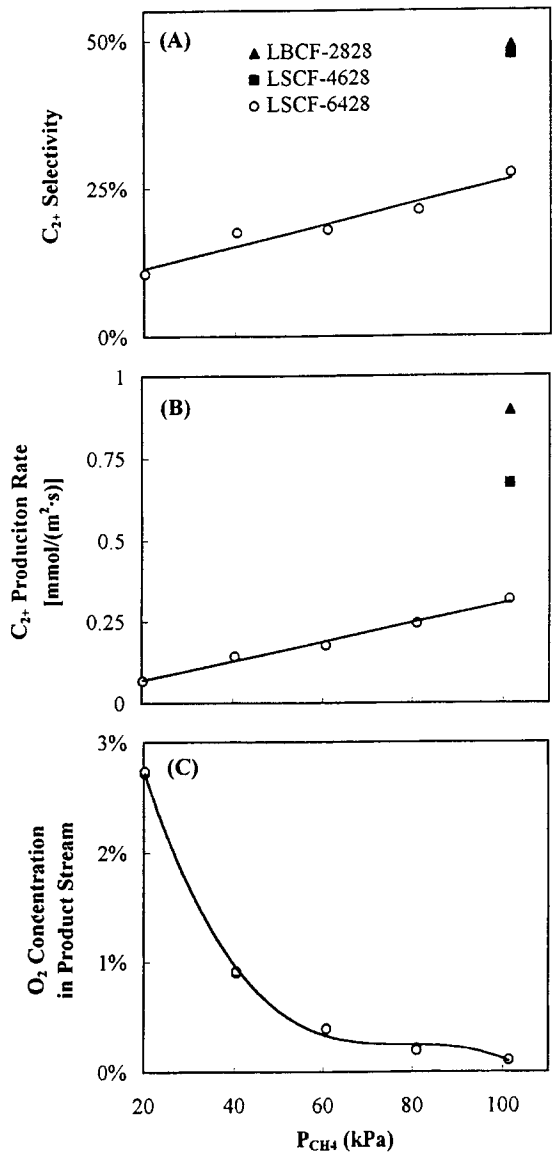

Figure 3. Effect of P_{CH_4} [$T = 1{,}098$ K, $F_{CH_4+He} = 166$ mmol/(m²·s), $P_{O_2} = 101$ kPa].

greater degree. This produces molecular oxygen in the gas phase, which then combusts C_2 products and lowers C_2 selectivity.

Of particular interest in Figure 3 is the linear dependence of selectivity and the C_{2+} production rate on P_{CH_4} for LSCF-6428. Selectivities increased from 10% to almost 30% as P_{CH_4} was increased from 20 kPa to 101 kPa. A the same time that measured O_2 concentrations in the exit, the methane stream dropped by a factor of 3. These observations imply that there is insufficient methane surface coverage, allowing oxygen ions to recombine into gaseous oxygen. The observation that selectivity increases linearly with P_{CH_4} points to increased methane chemical adsorption on the membrane surface, allowing more oxygen ions to react with methane to generate free methyl radicals, and resulting in a lower oxygen-ion recombination rate. Obviously, the measured oxygen concentration in the product stream from the reactor was not the total amount of oxygen recombined, because some portion of the recombined oxygen undergoes combustion with the C_{2+} products. This explains why the selectivity of LSCF-6428 was so low ($< 30\%$) even with a 0.08% outlet oxygen concentration. A similar dependency of selectivity and CH_4 conversion on P_{CH_4} was also observed by ten Elshof et al. (1995a) on LSCF-6482 at 1153 K.

The fact that selectivities and production rates of LBCF-2828 and LSCF-4628 were much higher than the values of LSCF-6428 under identical reaction conditions, suggests that the membrane surface structure plays a critical role in achieving a highly selective OCM reaction. Both LBCF-2828 and LSCF-4628 have higher oxygen vacancies than does LSCF-6428. Not only does this promote oxygen-ion transport through the membrane, but it also increases the activation of methane molecules. Thus, improvements in the catalytically selective surface is as important as the development of membranes with high oxygen-ion conductivities.

Dependence on temperature

In a previous study of LSCF-6482 for OCM, ten Elshof et al. (1995a) found that the thermal decomposition of methane to form H_2 took place at temperatures greater than 1,123 K. Because the appearance of H_2 could adversely affect the catalytic performance of these membranes in terms of its strong reduction potential, temperatures in this study were kept below 1,123 K. In fact, hydrogen was not detected at levels above ~ 0.3% during a prolonged experiment with LSCF-6428 at 1,103 K. This is consistent with a study by Tsai et al. (1996) on an LBCF-2828 membrane at 1,123 K.

Figure 4 shows the influence of the temperature on C_{2+} activity, selectivity, and oxygen flux for LBCF-2828 at $P_{CH_4} =$ 101 kPa and $P_{O_2} = 101$ kPa. As shown in Figure 4b, the oxygen flux experiences a sudden increase at about 1,048 K, indicating that temperatures greater than 1,048 K are required for these perovskite membrane disks to be oxygen-ion conductive. The results also show a linear dependence of C_{2+} selectivity on temperature and significant increases in the C_{2+} production rate at temperatures higher than 1,048 K (Figure 4a).

The linear increase of selectivity with escalating temperatures points to the effective inhibition of C_{2+} product combustion when using a membrane reactor configuration. In fact,

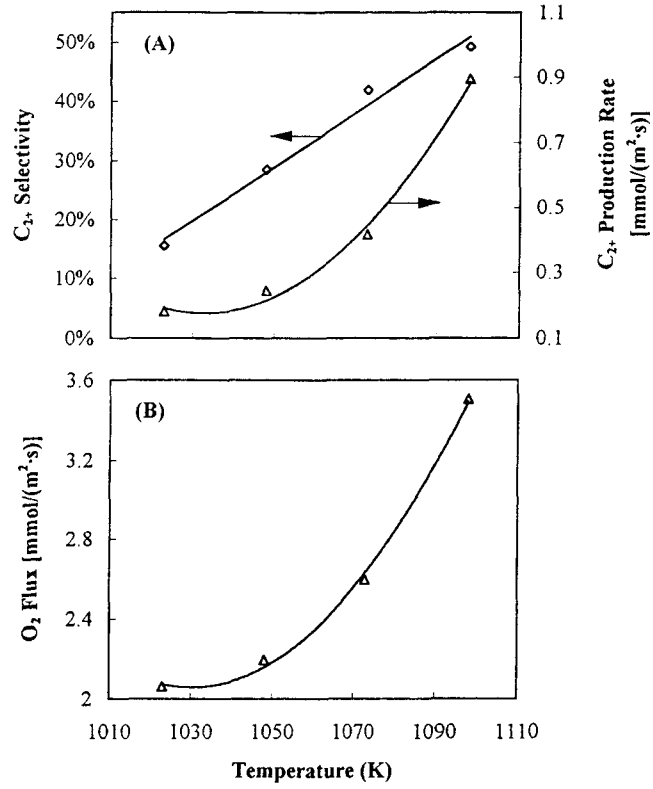

Figure 4. Influence of temperature (LBCF-2828, $P_{CH_4} = P_{O_2} = 101$ kPa).

Xu (1994) observed that C_{2+} selectivities started to level at about 1023 K for most of the 19 different OCM catalysts tested when methane and oxygen were co-fed in a packed-bed reactor. In other words, the combustion reaction, which is more thermodynamically favorable at high temperatures, was greatly restrained thanks to the low gas oxygen concentration, and consequently selectivities continued to increase even at 1,098 K. Studies by ten Elshof et al. (1995a) showed that LSCF-6482 reached its highest selectivity (62.7%) at 1,120 K and after this point, selectivity was reduced dramatically. They attributed this to the occurrence of methane decomposition at the higher temperatures used in their study.

According to Machin et al. (1992), the surface methyl radical-generation reaction is temperature-dependent and dramatically slower than the temperature-independent radical-coupling reaction in the gas phase. Based on their observations it can be inferred that, in the absence of combustion, the C_{2+} production rate is limited by the generation rate of free methyl radicals and can be increased by increasing the temperature. At low temperatures such as 1,023 K, active sites were less active, but there was still a significant flux of oxygen ions [~ 2.1 mmol/(m^2·s) for LBCF-2828] conducted through the membrane. In this case, most of the ions do not generate methyl radicals but recombine to gaseous oxygen and cause combustion, resulting in low selectivities at the lower temperatures.

While selectivity is the representation of the characteristics of the membrane surface, the C_{2+} production rate will depend on the combined effects of surface catalytic activation of methane and bulk oxygen-ion conductivity of the mem-

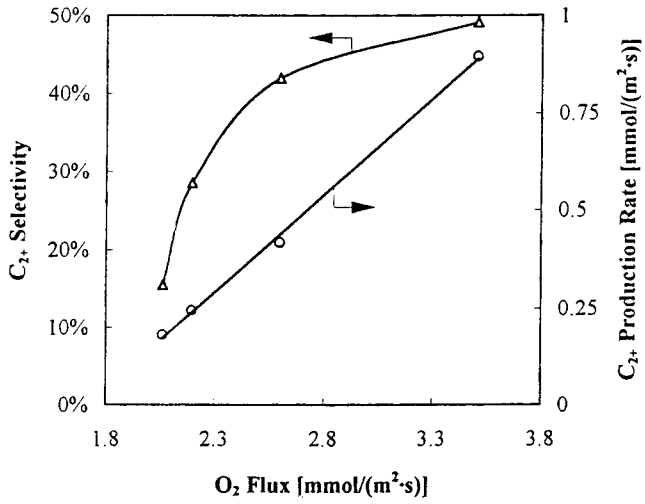

Figure 5. Influence of oxygen flux (LBCF-2828, T = 1,023 ~ 1,098 K).

brane. As shown in Figure 4a, the dramatic increase in the production rate of LBCF-2828 at temperatures higher than 1,048 K reflected this combined effect—greatly improved selectivity and oxygen ion flux. The direct correlation between selectivity (as well as C_{2+} production rate) and oxygen flux is demonstrated in Figure 5 at temperatures between 1,023 and 1,098 K. The selectivity curve in this figure clearly shows that selectivity increases rapidly with oxygen flux at lower values of oxygen flux (lower temperatures), but tends to level off at high oxygen flux levels. Apparently the activation energy for oxygen-ion recombination (Reaction H) is higher than the OCM activation energy. That is, at higher oxygen fluxes (higher temperatures) the recombination rate increases faster than does the OCM rate. As can be seen by the lower line in Figure 5, the latter has a linear dependence on oxygen flux over the entire oxygen flux (temperature) range. The implication here is that in order to maintan *both* high selectivity and high reactivity, it is necessary to increase the OCM rate independent of the oxygen recombination rate.

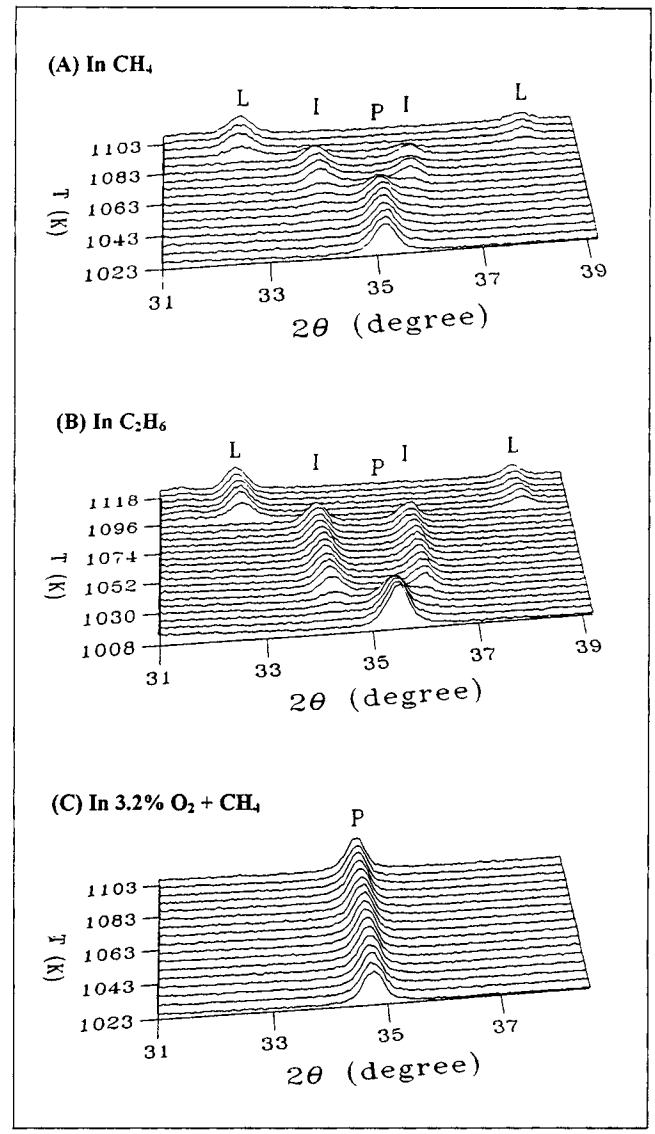

Figure 6. DXRD results for LSCF-6428 (P = LSCF-6428, I = intermediate state, L = La_2O_3).

Perovskite reduction by methane and ethane

While the data shown in Figures 3 and 4 were from disks that maintained their stability for times as long as 30 h, the disk developed "cracks" when attempts were made to raise the methane pressures above 101 kPa, and no useful data were obtained at these higher pressures. Because of the known susceptibility of these materials to become unstable when exposed to reducing gases at high temperatures, a separate reduction study was undertaken. This was accomplished by two methods: *in-situ* DXRD experiments of the powders under the same reaction conditions as used in activity tests, and XPS studies of the disks immediately after exposure to methane.

The most stable of the three perovskites is LSCF-6428 and Figures 6a and 6b show the DXRD results when this material (powder) was exposed to 101 kPa of methane (Figure 6a) and ethane (Figure 6b), respectively, while the temperature was ramped at 1.2 K/min from 1,008 K to 1,118 K. The changes in the peak area for the different phases in both methane and ethane are each plotted in Figure 7. As can be seen, the perovskite powder begins to reduce at about 1023 K in methane or ethane, indicating that the reductivity of methane and ethane are strong enough to cause phase changes in these perovskite oxides at high temperatures. The phase transformation occurs in two steps with the perovskite forming an intermediate phase, which subsequently transforms into La_2O_3 at about 1,083 K. As shown in Figure 7, it was also observed that the reductivity of ethane was even stronger than that of methane because the disappearance of the perovskite phase in ethane was earlier (1,013 K vs. 1,033 K) and faster (lasting 17 min vs. 30 min) than that in methane.

Figure 6c shows a plot of an identical experiment, but in a gas mixture consisting of CH_4 and O_2 with an oxygen concentration of only 3.2%. In this case, the perovskite remains stable, indicating that the presence of a small amount of oxygen inhibits reduction. Based on these observations, it is likely that the cracks in the membrane disks are due to methane

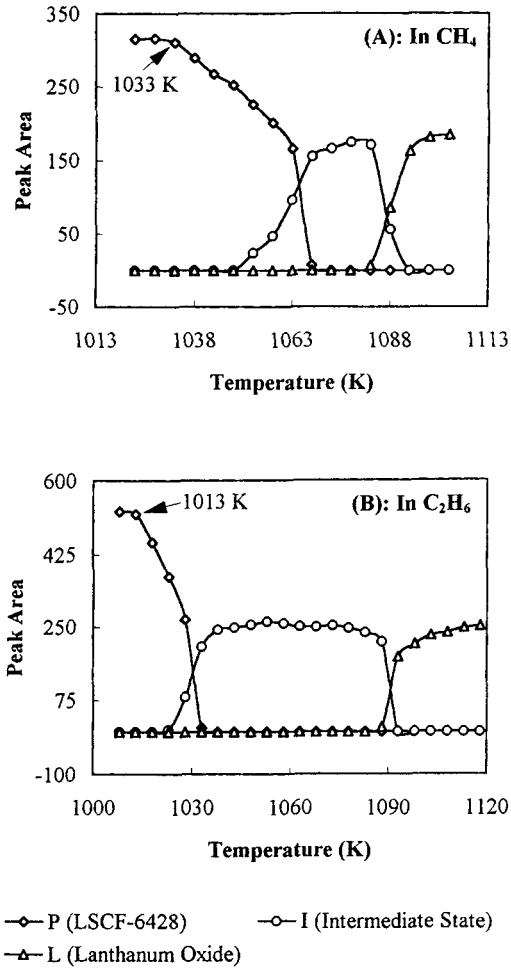

Figure 7. DXRD peak area as a function of temperature.

and C_{2+} reduction as a result of insufficient oxygen supply. The fact that so many of the disks were stable is probably due to the high rate of oxygen-ion recombination at the reactive side of the membrane, which resulted in bulk oxygen concentrations between 0.5 and 3% (see Figure 3d).

The same DXRD experiments were also conducted on LSCF-4628 and LBCF-2828, and similar results were observed. The DXRD results with the powders were confirmed by separate XPS experiments on the perovskite disks. In this case, when an LSCF-6428 disk was exposed to pure methane at 973 K, surface oxygen measurements indicated the presence of surface cracks in the disk, which were then visually corrobated. Thus, surface cracks can develop at even lower temperatures if there is insufficient oxygen present. It should also be pointed out that, in some perovskite systems, H_2O can be damaging, particularly at low temperatures. However, at the temperatures used here, there was no apparent influence of H_2O.

Conclusions

The results of this study clearly demonstrate that when [La/Sr] [Co/Fe] perovskite materials are configured as catalytic membranes, there are significant improvements in OCM selectivities and C_2 production rates from those observed with these materials in a conventional packed-bed reactor. However, the highest measured selectivities were only 50%, and this is attributed to high oxygen-ion recombination rates that lead to the formation of gaseous oxygen on the methane side of the membrane, and subsequently to undesired combustion of the C_2 products in the gas phase. Interestingly, the oxygen-ion diffusion rates do not appear to be limiting with these materials. The total oxygen flux increased by factors of 3–5 when methane replaced nitrogen on the low oxygen side of the membrane, indicating that the OCM reaction served to increase the consumption of the oxygen ions arriving at that surface. However, while the total oxygen flux in the presence of methane increased with higher oxygen pressures on the high oxygen side of the membrane, C_{2+} selectivities remained the same. This indicates that the oxygen-ion recombination rate is still too highly and successfully competes with the OCM reaction.

The effects of temperature and methane pressure were studied in an attempt to determine their influence on the rates of these two competing reactions. While increasing temperatures produced higher OCM rates, it was found that the activation energy of the recombination reaction was higher than that of the OCM reaction, so that its rate increased faster than the OCM rate at temperatures above about 1073 K (Figures 4 and 5). Increasing the methane pressure on the reactive side of the membrane did preferentially increase the OCM reaction rate and also the selectivity (Figures 3a and 3b). A natural extension of this result is to use even higher methane pressures, as long as the perovskites can remain stable in the presence of reducing gases at higher pressures. When the three perovskites were subjected to *in situ* DXRD experiments in the presence of CH_4 and C_2H_6, they all underwent marked phase transformations as a result of reduction at temperatures above 1023 K. Reduction susceptibility was higher with the LSCF-4628 and LBCF-2828 and in ethane vs. methane. However, these materials were totally stable at these temperatures in the presence of small concentrations of oxygen.

The results presented here have a number of implications. First of all, if these materials are going to be practical as membrane reactors for commercial OCM processes (high activities at high selectivities), it is necessary that OCM catalytic activity be increased *without* increasing the oxygen-ion recombination reactivity. High selectivities can only be achieved if there is a balance between the oxygen flux arriving at the reactive surface and the OCM reaction rate, and then only if the OCM rate is higher than the oxygen-ion recombination rate. An additional unknown factor here is whether such conditions will lead to reduction of these materials since, ideally, there would only be sufficient oxygen present to activate methyl radicals. The results here show that these materials are stable in the presence of co-fed oxygen, but the required minimum oxygen concentrations are not known and it is not clear whether oxygen ions supplied through the membrane are as stabilizing as gaseous oxygen.

In summary, the following conclusions have been reached:

1. The combustion of C_2 hydrocarbons, the primary competing reaction, does not take place on the perovskite membrane surface. This presents a strong argument for using these materials in a membrane configuration for OCM reaction.

2. Compared with a fixed-bed configuration under identical conditions, LSCF and LBCF perovskite membranes can be used to dramatically improve C_2 selectivity by a factor of 4 and C_2 production rate (on a per-unit-area basis) by a factor of 7.

3. C_2 selectivity limitations are attributed to high oxygen-ion recombination rates, which not only competes with surface methane activation reaction but leads to the formation of gaseous oxygen and subsequent combustion of C_2 hydrocarbons at the methane side of the membrane.

4. The results obtained at varying temperatures and methane pressures clearly show that the strategies to improve C_2 selectivity and production rate should concentrate on increasing the OCM rate independent of the oxygen recombination rate.

5. DXRD experiments have shown that the stability of LSCF perovskites under OCM reactions can be maintained as long as there is a sufficient concentration of oxygen near the surface. For example, 3% bulk oxygen concentration was effective in these studies to maintain LSCF stability in 97 kPa of methane at temperatures up to 1,100 K.

Acknowledgment

This material is based on work supported by the National Science Foundation under Grant CTS-9521721. The authors also thank Dr. Jeffry Stevenson and Nancy Colton from Pacific Northwest National Laboratory (PNNL) for their help in preparing the perovskite disk membranes, and Dr. Chuck Peden of PNNL for his assistance with the XPS experiments.

Notation

C_{2+} = hydrocarbons with more than one carbon in molecule
F_i = flow rate of species i, $\text{mmol}\cdot\text{m}^{-2}\cdot\text{s}^{-1}$
h = quasi-free hole in the valence band
J_{O_2} = oxygen flux through membrane, $\text{mmol}\cdot\text{m}^{-2}\cdot\text{s}^{-1}$
k_i = reaction-rate constant for reaction i
P_i = partial pressure of i, kPa
X_i = conversion of species i, %

Literature Cited

Alcock, C. B., J. J. Carberry, R. Doshi, and N. Gunasekaran, "Coupling Reaction on Oxide Solid Solution Catalysts," *ACS Preprints-Symposia*, **37**(1), 123 (1992).

Andersen, A. G., T. Hayakawa, K. Suzuki, M. Shimizu, and K. Takehira, "Electrochemical Methane Conversion over $SrFeO_{3-\delta}$ Perovskite on an Yttrium Stabilized Zirconia Membrane," *Catal. Lett.*, **27**, 221 (1994).

Baronetti, G. T., C. Padro, O. A. Scelza, A. A. Castro, V. C. Corberan, and J. L. G. Fierro, "Structure and Reactivity of Alkali-Doped Calcium-Oxide Catalysts for Oxidative Coupling of Methane," *Appl. Catal. A*, **101**, 167 (1993).

Barrault, J., C. Grosset, M. Dion, M. Ganne, and M. Tournoux, "Lamellar Perovskites M^I ($A_{n1}B_nO_{3n+1}$) Catalysts for Oxidative Coupling of Methane," *Appl. Catal. A*, **88**, 179 (1992).

Bouwmeester, H. J. M., H. Kruidhof, and A. J. Burggraaf, "Importance of the Surface Exchange Kinetics as Rate Limiting Step in Oxygen Permeation Through Mixed-Conduction Oxides," *Solid State Ionics*, **72**, 185 (1994).

Buyevskaya, O. V., M. Rothaemel, H. W. Zanthoff, and M. Baerns, "Transient Studies on the Role of Oxygen Activation in the Oxidative Coupling of Methane over Sm_2O_3 Sm_2O_3/MgO and MgO Catalytic Surfaces," *J. Catal.*, **150**, 71 (1994).

Chick, L. A., L. R. Pederson, G. D. Maupin, J. L. Bates, L. E. Thomas, and G. J. Exarhos, "Glycine-Nitrate Combustion Synthesis of Oxide Ceramic Powders," *Mater. Lett.*, **10**(1-2), 6 (1990).

Choudhary, V. R., V. H. Rane, and R. V. Gadre, "Influence of Precursors Used in Preparation of MgO on Its Surface-Properties and Catalytic Activity in Oxidative Coupling of Methane," *J. Catal.*, **145**, 300 (1994).

Driscoll, D. J., K. D. Campbell, and J. H. Lunsford, "Surface-Generated Gas-Phase Radicals: Formation, Detection, and Role in Catalysis," *Adv. Catal.*, **35**, 139 (1987).

Dubois, J. L., and C. J. Cameron, "Common Features of Oxidative Coupling of Methane Cofeed Catalysts," *Appl. Catal.*, **67**, 49 (1990).

Feng, Y., J. Niiranen, and D. Gutman, "Kinetic Studies of the Catalytic Oxidation of Methane: 2. Methyl Radical Recombination and Ethane Formation over 1% Sr/La_2O_3," *J. Phys. Chem.*, **95**, 6564 (1991).

Grzybek, T., G. C. Maiti, D. Scholz, and M. Baerns, "Surface Composition and Selectivity of Sodium-Compound-Impregnated Calcium Oxide Catalysts for the Oxidative Coupling of Methane," *Appl. Catal. A*, **107**, 115 (1993).

Hayakawa, T., H. Orita, M. Shimizu, K. Takehira, A. G. Andersen, K. Nomura, and Y. Ujihira, "Oxidative Coupling of Methane over $LaCoO_{3-\delta}$-Based Mixed Oxides," *Catal. Lett.*, **16**, 359 (1992).

Kaminsky, M. P., G. W. Zajac, J. C. Campuzano, M. Faiz, L. Beaulaigue, K. Gofron, G. Jennings, J. M. Yao, and D. K. Saldin, "Oxygen X-Ray Absorption Near-Edge Structure Characterization of the Ba-Doped Yttria Oxidative Coupling Catalyst," *J. Catal.*, **136**, 16 (1992).

Kröger, F. A., *The Chemistry of Imperfect Crystals*, 2nd ed., North-Holland, Amsterdam (1974).

Kruidhof, H., H. J. M. Bouwmeester, R. H. J. E. van Doorn, and A. J. Burggraaf, "Influence of Order-Disorder Transitions on Oxygen Permeability Through Selected Nonstoichiometric Perovskite-Type Oxides," *Solid State Ionics*, **63**(65), 816 (1993).

Lacombe, S., H. Zanthoff, and C. Mirodatos, "Oxidative Coupling of Methane over Lanthana Catalysts. II. A Mechanistic Study Using Isotope Transient Kinetics," *J. Catal.*, **155**, 106 (1995).

Lin, Y. S., and Y. Zeng, "Catalytic Properties of Oxygen Semipermeable Perovskite-Type Ceramic Membrane Materials for Oxidative Coupling of Methane," *J. Catal.*, **164**, 220 (1996).

Ling, S., M. P. Anderson, and T. A. Ramanarayanan, "Optimization of Ionic Transport Through Mixed Conducting Oxide Ceramics," *Solid State Ionics*, **59**, 33 (1993).

Lunsford, J. H., "The Role of Surface-Generated Gas-Phase Radicals in Catalysis," *Langmuir*, **5**, 12 (1989).

Machin, I., P. Pereira, de V. Gouveia, and F. Rosa, "Modeling of Catalytic Oxidative Coupling of Methane," *ACS Preprints-Symposia*, **37**(1), 173 (1992).

Omata, K., S. Hashimoto, H. Tominaga, and K. Fujimoto, "Oxidative Coupling of Methane Using a Membrane Reactor," *Appl. Catal.*, **52**, L1 (1989).

Peng, X. D., and P. C. Stair, "The Active Phase in Sodium-Doped Calcium Oxide Catalysts for Oxidative Coupling of Methane," *J. Catal.*, **128**, 264 (1991).

Reyes, S. C., E. Iglesia, and C. P. Kelkar, "Kinetic-Transport Models of Bimodal Reaction Sequences. 1. Homogeneous and Heterogeneous Pathways in Oxidative Coupling of Methane," *Chem. Eng. Sci.*, **48**, 2643 (1993).

Squire, G. D., H. Luc, and D. C. Puxley, "In Situ X-Ray Diffraction Study of Lanthanum Oxide Catalysts During the Oxidative Coupling of Methane," *Appl. Catal. A*, **108**, 261 (1994).

Steele, B. C. H., "Oxygen Ion Conductors and Their Technological Applications," *Mater. Sci. Eng.*, **B13**, 79 (1992).

Tang, C. L., J. L. Zang, and L. W. Lin, "Roles of Oxygen and Carbon-Dioxide on Methane Oxidative Coupling over CaO and Sm_2O_3 Catalysts," *Appl. Catal. A*, **115**, 243 (1994).

ten Elshof, J. E., H. J. M. Bouwmeester, and H. Verweij, "Oxidative Coupling of Methane in a MIxed-Conducting Perovskite Membrane Reactor," *Appl. Catal. A*, **130**, 195 (1995a).

ten Elshof, J. E., B. A. van Hassel, and H. J. M. Bouwmeester, "Activation of Methane Using Solid Oxide Membranes," *Catal. Today*, **25**, 397 (1995b).

Teraoka, Y., H. M. Zhang, K. Okamoto, and N. Yamazoe, "Mixed Ionic-Electronic Conductivity of $La_{1-x}Sr_xCo_{1-y}Fe_yO_{3-\delta}$ Perovskite-Type Oxides," *Mater. Res. Bull.*, **23**, 51 (1988).

Teraoka, Y., H. M. Zhang, S. Furukawa, and N. Yamazoe, "Oxygen Permeation through Perovskite-Type Oxides," *Chem. Lett.*, 1743 (1985).
Tsai, C. Y., Y. H. Ma, W. R. Moser, and A. G. Dixon, "The Evaluation of Perovskite Membrane Reactors for the Partial Oxidation of Methane to Synthesis Gas," *Preprints, 5th World Congr. Chem. Eng.*, San Diego (1996).
Tung, W. Y., and L. L. Lobban, "Oxidative Coupling of Methane over Li/MgO: Kinetics and Mechanisms," *Ind. Eng. Chem. Res.*, **31**, 1621 (1992).
Wagner, C., *Atom Movements*, ASM, Cleveland, p. 153 (1951).
Wang, W., and Y. S. Lin, "Analysis of Oxidation Coupling of Methane in Dense Oxide Membrane Reactors," *J. Membr. Sci.*, **103**, 219 (1995).
Xu, S. J., *Catalysts for the Oxidative Coupling of Methane*, MS Thesis, Washington State University, Pullman (1994).
Zhang, Z. L., and M. Baerns, "Oxidative Coupling of Methane over $CaO-CeO_2$ Catalysts: Effect of Oxygen-Ion Conductivity on C_2 Selectivity," *J. Catal.*, **135**, 317 (1992).

Manuscript received Oct. 28, 1996, and revision received Apr. 4, 1997.